blood®
Regular Article

THROMBOSIS AND HEMOSTASIS

Single-molecule imaging of von Willebrand factor reveals tension-dependent self-association

Hongxia Fu,[1-7,*] Yan Jiang,[1-3,*] Wesley P. Wong,[1-3] and Timothy A. Springer[1-3]

[1]Program in Cellular and Molecular Medicine, Boston Children's Hospital, Boston, MA; [2]Department of Biological Chemistry and Molecular Pharmacology, and [3]Department of Pediatrics, Harvard Medical School, Boston, MA; [4]Division of Hematology, Department of Medicine, [5]Institute for Stem Cell and Regeneration Medicine, and [6]Department of Bioengineering, University of Washington, Seattle, WA; and [7]Bloodworks Northwest Research Institute, Seattle, WA

KEY POINTS

- **Hydrodynamic drag on tethered VWF induces elongation and imparts mechanical tension that activates binding of free VWF at a tension of 10 pN.**
- **Decrease in flow and hence tension on tethered VWF reverses VWF self-association.**

von Willebrand factor (VWF) is an ultralong concatemeric protein important in hemostasis and thrombosis. VWF molecules can associate with other VWF molecules, but little is known about the mechanism. Hydrodynamic drag exerts tensile force on surface-tethered VWF that extends it and is maximal at the tether point and declines linearly to 0 at the downstream free end. Using single-molecule fluorescence microscopy, we directly visualized the kinetics of binding of free VWF in flow to surface-tethered single VWF molecules. We showed that self-association requires elongation of tethered VWF and that association increases with tension in tethered VWF, reaches half maximum at a characteristic tension of ~10 pN, and plateaus above ~25 pN. Association is reversible and hence noncovalent; a sharp decrease in shear flow results in rapid dissociation of bound VWF. Tethered primary VWF molecules can recruit more than their own mass of secondary VWF molecules from the flow stream. Kinetics show that instead of accelerating, the rate of accumulation decreases with time, revealing an inherently self-limiting self-association mechanism. We propose that this may occur because multiple tether points between secondary and primary VWF result in lower tension on the secondary VWF, which shields more highly tensioned primary VWF from further association. Glycoprotein Ibα (GPIbα) binding and VWF self-association occur in the same region of high tension in tethered VWF concatemers; however, the half-maximal tension required for activation of GPIbα is higher, suggesting differences in molecular mechanisms. These results have important implications for the mechanism of platelet plug formation in hemostasis and thrombosis.

Introduction

In the arterial circulation, the glycoprotein von Willebrand factor (VWF) is of central importance in hemostasis and thrombosis. VWF is biosynthesized as concatemers consisting of variable numbers of covalently linked monomers.[1,2] VWF concatemers are transiently attached to the endothelial cell surface during secretion and then circulate in blood plasma and attach to the subendothelial matrix at sites of injury.[1-5] Surface-tethered VWF can be activated by elevated shear stress to bind the platelet membrane glycoprotein Ibα (GPIbα) receptor.[6,7] Surface-tethered VWF may also associate with circulating VWF, a process known as intermolecular self-association.[8-14] Association of circulating VWF not only amplifies the amount of tethered VWF available to bind GPIbα to support platelet adhesion,[8] but it also enhances platelet activation.[12] VWF self-association thus contributes to platelet adhesion and aggregation during thrombus formation and is an important therapeutic target for hemostasis and thrombosis.[15,16]

Despite progress in understanding VWF self-association, the molecular mechanisms and force requirements for self-association remain unclear. Higher shear stress has been found to induce a greater amount of binding between circulating and surface-attached VWF,[9] but self-association has also been observed in static conditions.[10] By using single-molecule imaging, we showed that shear flow induces surface-tethered VWF to elongate from a compact to a linear form, and at higher flow rates, the mechanical tension within VWF increases sufficiently to bind GPIbα from the flow stream.[6,7] One possibility is that VWF elongation and mechanical tension also activate association with VWF in the flowstream, but direct evidence for this hypothesis is currently lacking.

To date, association between surface-attached and circulating VWF has been studied at the macroscopic level using bulk VWF preparations, but such studies average the behavior of samples containing VWF concatemers of a wide range of sizes, each of which experiences a different force history.[8-14] To achieve quantitative insights into the mechanism and force-dependence of

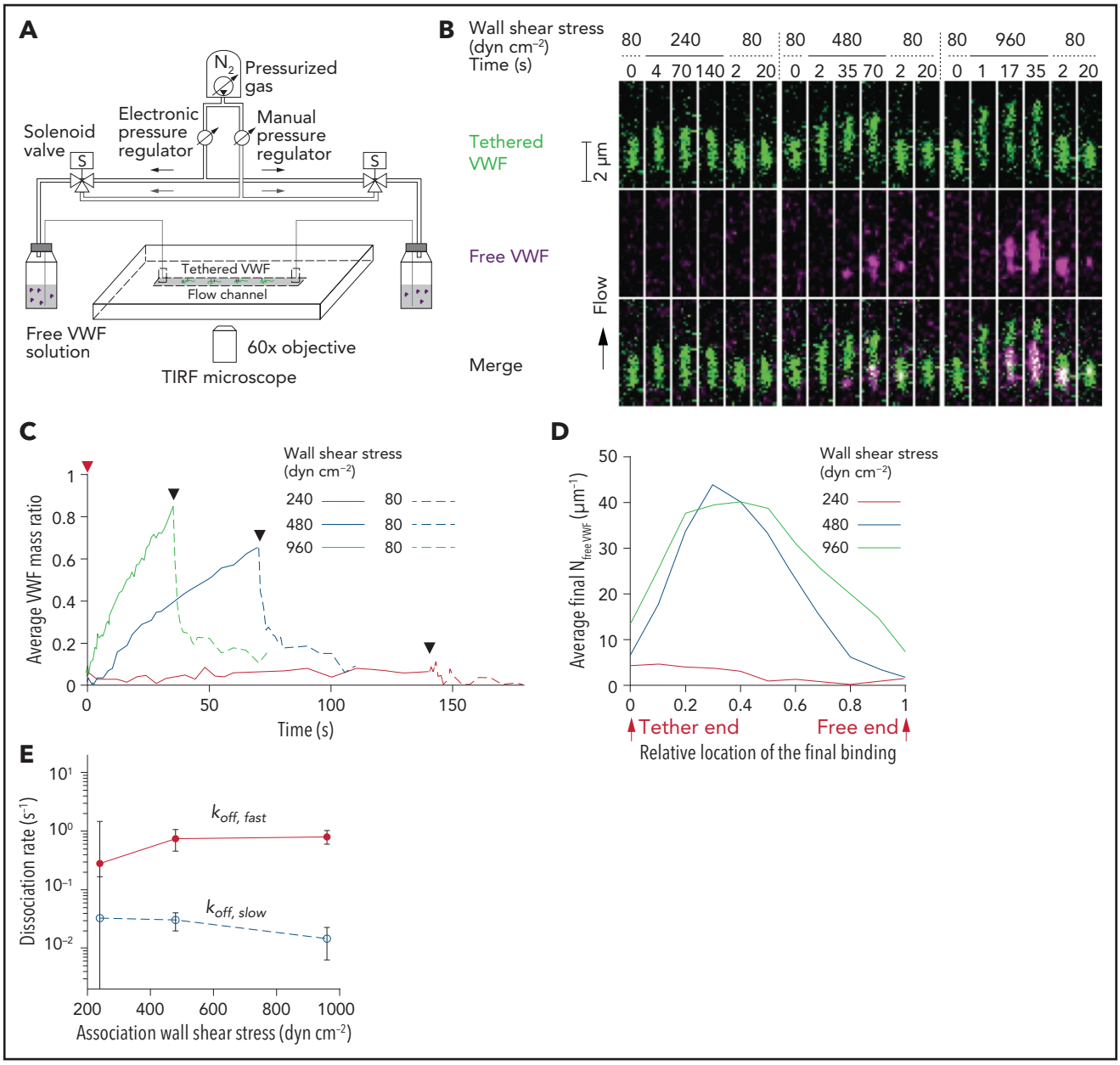

Figure 1. Association of VWF in flow to tethered VWF. (A) Schematic of total internal reflection fluorescence (TIRF) microscopy with air pressure-actuated flow. (B) Dual-color fluorescence images showing the extension and relaxation of a representative tethered Alexa Fluor 488–labeled VWF molecule and the binding and dissociation of Alexa Fluor 647–labeled VWF in flow at the indicated wall shear stresses. (C) Average time course of free VWF association to single tethered VWF concatemers. The y-axis is the mass ratio of bound VWF:tethered VWF. The red triangle marks the increase in flow from 80 dyn cm^{-2} to the shear rate keyed by color, and black triangles mark resumption of flow at 80 dyn cm^{-2}. (D) Profile of final VWF binding density at relative locations along individual tethered VWF concatemers. $N_{freeVWF}$ is the monomer number of bound VWF. (E) Dissociation rate at 80 dyn cm^{-2} of VWF that had been bound at different wall shear stresses. Dissociation in (panel C) was fit to a double exponential function $R_{freeVWF}(t) = R_{freeVWF,fast} \cdot \exp(-k_{off,fast} \cdot t) + R_{freeVWF,slow} \cdot \exp(-k_{off,slow} \cdot t)$. In panels C-E, binding of free VWF (10 μg mL^{-1}) was measured on 93 tethered VWF molecules. The average end-to-end distance of these VWF molecules was 3.6 ± 1.1 μm at 960 dyn cm^{-2}, and they contained 149 ± 32 monomers based on integrated fluorescence intensity.

VWF self-association, we have measured VWF self-association kinetics within elongated, tethered, single VWF molecules and revealed their dependence on tension.

Methods

Recombinant VWF, GPIbα, and the flow system

Recombinant human VWF was labeled with Alexa Fluor 488 and biotin, purified by using size exclusion chromatography, and attached to the wall of flow channels coated with polyethylene glycol (PEG) and PEG-biotin.[6] Recombinant human VWF or GPIbα for use in the flow stream were labeled with Alexa Fluor 647.[6,7,17] The microfluidic flow channel was mounted on a total internal reflection fluorescence (TIRF) microscope (Figure 1A). VWF or GPIbα were introduced into nitrogen-pressurized vials at one end of the flow chamber at 80 dyn cm^{-2} and switched at the speed of sound without introducing flow rate spikes by automatically actuated sequential changes

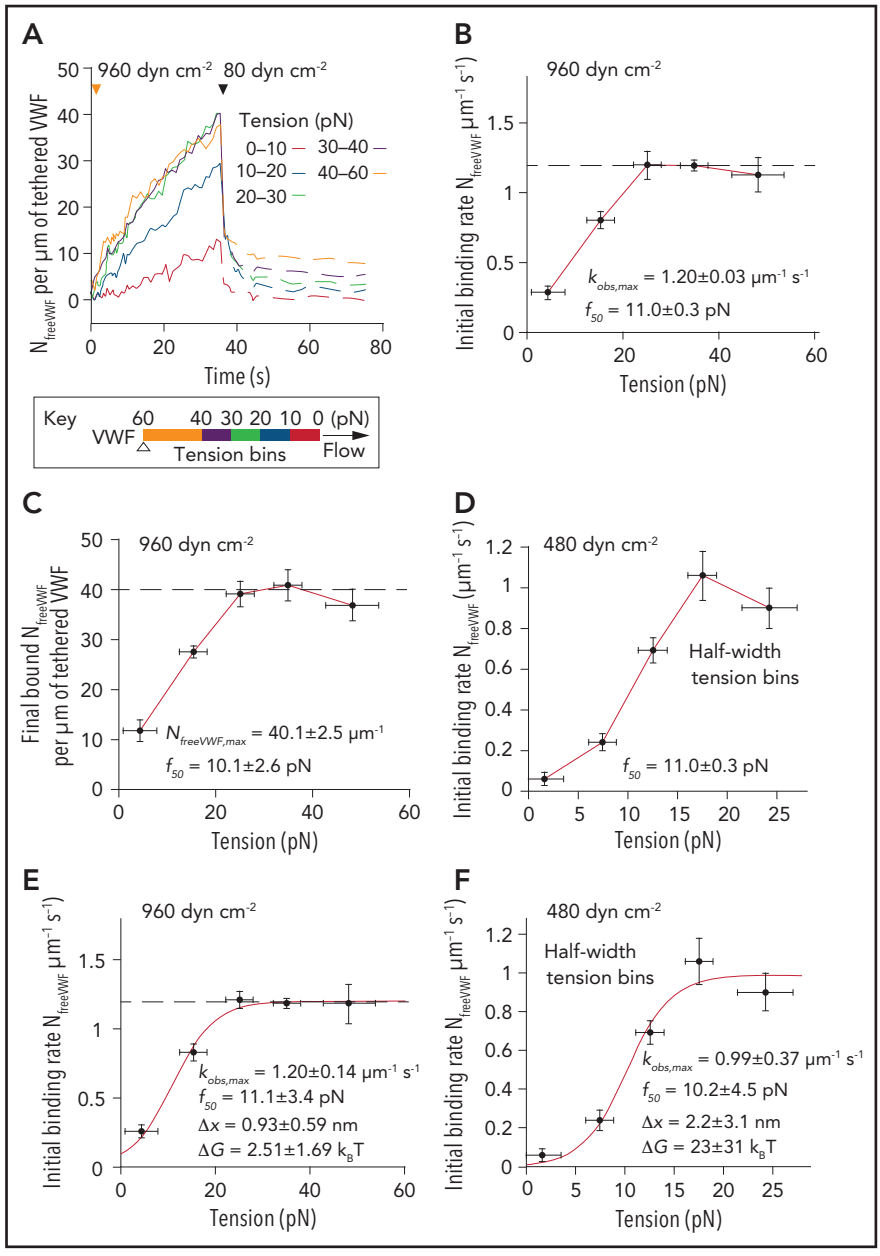

Figure 2. Tension-regulated VWF self-association. (A) Average time course of VWF (10 µg mL^{-1}) binding to single tethered VWF concatemers at 960 dyn cm^{-2}. Curves show association (solid lines) and dissociation (dashed lines) at 80 dyn cm^{-2} and are color coded by tension bin as shown in the key (the triangle shows the tether point). Data are averaged from 62 tethered VWF molecules used in Figure 1C-E that are large enough to include a 40-to-60 pN tension bin at 960 dyn cm^{-2}. (B) Initial VWF binding rate and (C) final bound density of VWF from data in panel A. In panels B and C, the maximum binding rate and total binding density are estimated as the average of the values in the 20-to-30 and 30-to-40 pN bins. The force at half-maximal binding, f_{50}, was determined as the intercept of the half maxima with the lines drawn through the data points on either side of the half maxima. (D) Initial binding rate of VWF (10 µg mL^{-1}) at 480 dyn cm^{-2} using smaller (5 pN) tension bins. In panels B-D, red lines connect neighboring points. (E-F) Fits of the data in panels B and D to a 2-state model (red lines) in which the observed initial binding rate $k_{obs} = k_{obs,max}/(1+\exp((\Delta G - f\cdot\Delta x)/k_BT))$, where $k_{obs,max}$ is the maximum observed initial binding rate, ΔG is the free energy difference between the 2 states (fast binding and slow or no binding), and Δx is the displacement along the force f direction between the 2 states. Data in panels A-F are from the same set of tethered VWF concatemers. In panels B-D, error bars represent standard deviation. In panels E-F, error bars represent standard deviation for tension and 95% confidence intervals for the other variables.

in nitrogen pressure to achieve flow rates of 240, 80, 480, 80, 960, and 80 dyn cm^{-2} at 21°C. Images with 0.007- to 0.008-second exposure times were acquired at frame rates of 0 .2 to 2 s^{-1} designed to minimize photobleaching (supplemental Tables 1 and 2 available on the *Blood* Web site).

Data analysis

Fluorescent images of multiple single tethered VWF molecules in each frame were analyzed using a custom-written MATLAB code.[6] VWF extension, mass, monomer number, and GPIbα number were calculated in each frame of movies on the basis of the contour and fluorescence intensity of primary tethered and secondary bound VWF or GPIbα molecules that had been standardized with the intensity of single Alexa Fluor 488 and Alexa Fluor 647 fluorophores and Alexa Fluor stoichiometry of coupling to VWF or GPIbα. Tension along tethered VWF was estimated by summing the drag force on all downstream VWF monomers that were modeled as a string of VWF domain

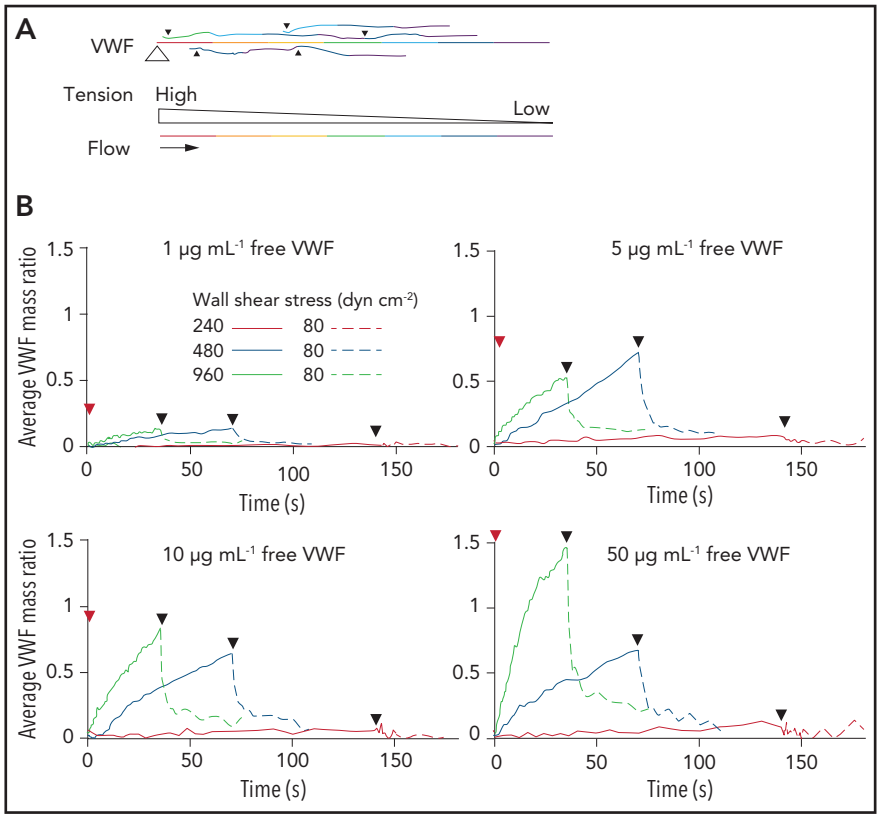

Figure 3. VWF self-association kinetics as a function of free VWF concentration and shear stress. (A) Scheme for VWF self-association. Top: A primary VWF molecule tethered on the substrate at the large open triangle is shown with secondary VWF molecules tethered at small closed triangles. Bottom: Key for the tension within each VWF molecule. (B) Average time course of VWF self-association after wall shear stress increase from 80 to 240, 480, or 960 dyn cm^{-2} (red arrows) and then decrease to 80 dyn cm^{-2} (black arrows) with 1, 5, 10, or 50 μg mL^{-1} free VWF. Different sets of tethered VWF molecules (in independent flow channels) were measured for each free VWF concentration; at each free VWF concentration, the same set of tethered VWF molecules was measured at each shear stress. Data were from 67, 70, 93, and 57 VWF molecules for 1, 5, 10, and 50 μg mL^{-1} free VWF, respectively. Data for 10 μg mL^{-1} free VWF are the same as in Figure 1C. Flow pattern, imaging exposure time, and frame rates are described in supplemental Tables 1 and 2.

beads.[6] The kinetics of free VWF or GPIbα binding were analyzed for each tension bin in tethered VWF molecules at different shear stresses. Additional details are provided in the supplemental Methods.

Results

VWF self-association in shear flow

To study VWF self-association in flow, we tethered recombinant human VWF labeled with Alexa Fluor 488 and biotin to a flow chamber wall coated with traptavidin.[6] Alexa Fluor 647–labeled free VWF at a physiologically relevant concentration of 10 μg mL^{-1}[18] (To separate the exponent and ref. 18, move ref. 18 to after "concentration".) was then infused at a wall shear stress of 80 dyn cm^{-2} with air pressure–actuated switching to intervening periods of flow at 240, 480, and 960 dyn cm^{-2} (Figure 1A-B).

Dual-color TIRF microscopy showed that tethered VWF was elongated at 80 dyn cm^{-2}, elongated further at 240, 480, and 960 dyn cm^{-2}, and rapidly relaxed to a shorter length upon return to 80 dyn cm^{-2} (Figure 1B). Very little free VWF bound to the elongated tethered VWF at 80 or 240 dyn cm^{-2}; however, much more binding occurred at 480 and 960 dyn cm^{-2} (Figure 1B-C). Free VWF preferentially bound near the VWF tether point on the substrate and bound further downstream along the length of the tethered VWF molecule at 960 dyn cm^{-2} compared with binding at 480 dyn cm^{-2} (Figure 1B,D).

Although ligand binding in stasis depends on diffusion for the encounter between the ligand and receptor, flow transports free VWF past tethered VWF and hence increases the encounter frequency. Therefore, we compared binding at 240, 480, and 960 dyn cm^{-2} as if it were completely transport-limited, that is, we compared binding over time interval lengths that were inversely related to shear such that the same number of free VWF molecules had flowed past in each case (Figure 1C). Increasing shear stress nonetheless increased VWF binding to tethered VWF, showing that increased binding was not the result of increased VWF transport. At 960 dyn cm^{-2}, the mass ratio of bound VWF to tethered VWF nearly equaled 1 (Figure 1C). Furthermore, the rate of binding increased with shear, as shown by comparing the slopes of the binding curves at 960, 480, and 240 dyn cm^{-2} (Figure 1C). These results suggest tension-dependent activation of binding of tethered VWF to VWF in the flow stream.

Shear dependence of free VWF binding to tethered VWF was further demonstrated by rapid dissociation of most of the bound VWF after decreasing the wall shear stress to 80 dyn cm^{-2} (Figure 1B-C). Fits assuming 2 populations of bound VWF molecules (double exponential decay) showed that most VWF molecules dissociated at a rate of ~0.8 s^{-1} and a smaller population

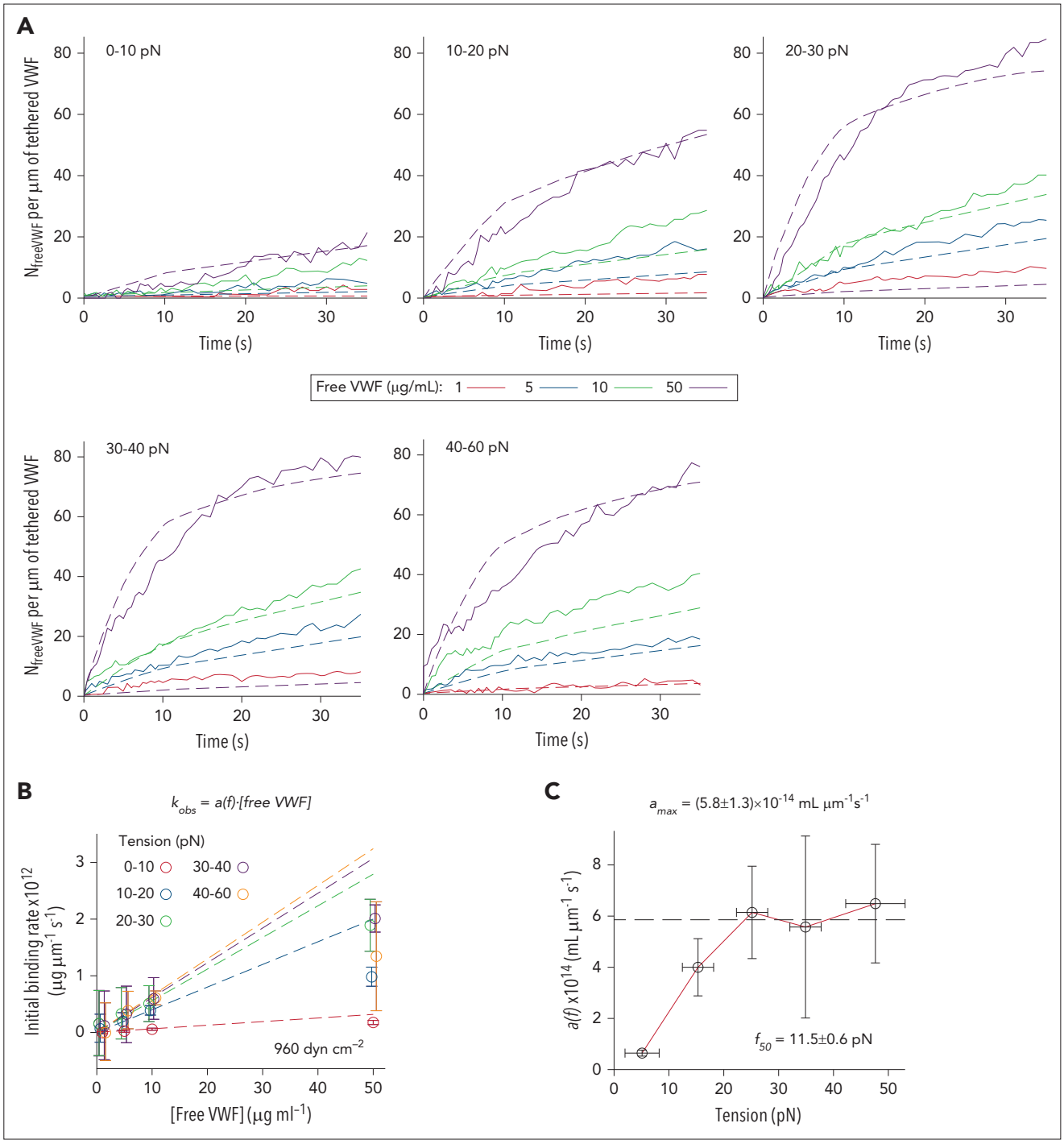

Figure 4. Dependence of VWF self-association on free VWF concentration. (A) Free VWF binding kinetics (solid lines) after flow increase from 80 to 960 dyn cm^{-2} at different concentrations of free VWF. For each tension bin, the curves were fitted using a homogeneous binding model assuming the free VWF molecules bind as individual monomers. Fitting to the following equation yielded the dissociation and association rate (k_{off} and k_{on}) for free VWF binding to regions of tethered VWF:[6] $N_{freeVWF} = N_{total} \cdot (1-\exp(-(k_{on}[C] + k_{off})\Delta t \cdot i)) \cdot k_{on}[C]/(k_{on}[C] + k_{off})$ where N_{total} is the total number of binding sites in tethered VWF that belong to the tension bin, $N_{freeVWF}$ is the monomer number of bound VWF in the same region, [C] is the concentration of free VWF monomers in solution, i is the frame number, and Δt is the time lag between consecutive frames. The predictions of the fitted model are shown in corresponding colors (dashed lines). Data for 1, 5, 10, and 50 µg mL^{-1} free VWF are with 52, 69, 62, and 51 tethered VWF concatemers, respectively, which were long enough to include a 40-to-60 pN tension bin. Data for 10 µg mL^{-1} free VWF are the same as in Figure 3. (B) Initial VWF binding rate per µm of tethered VWF in each tension bin at 960 dyn cm^{-2} wall shear stress (circles). The data points corresponding to the tension bins are jittered along the x-axis to avoid overlap. Dashed lines show linear fit (inset formula) to the data points from 1 to 10 µg mL^{-1} VWF, that is, with data at 50 µg mL^{-1} VWF omitted from the fit (see "Results"). a(f) is a tension-dependent, numerical fitting parameter. (C) Tension dependence of the a(f) value determined in (B). Red lines connect points.

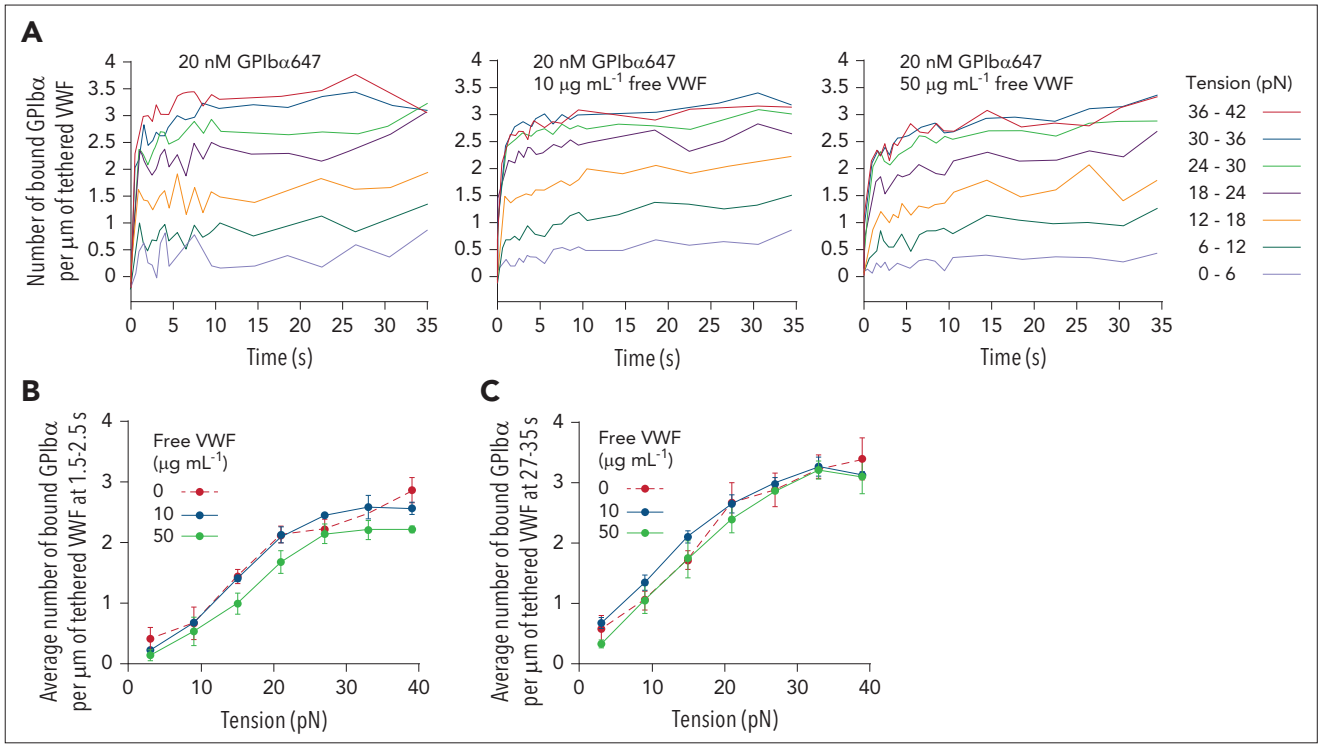

Figure 5. Effect of VWF self-association on GPIbα binding. (A) Time course of GPIbα647 binding to Alexa Fluor 488–labeled tethered VWF in the presence of 20 nM GPIbα647 and 0, 10, or 50 μg mL^{-1} of free unlabeled VWF at 960 dyn cm^{-2} wall shear stress. Tension bins are keyed according to color. (B-C) Number of bound GPIbα647 molecules averaged over time periods between (B) 1.5 and 2.5 seconds and (C) 27 and 35 seconds after the start of flow at 960 dyn cm^{-2}. Data for 0, 10, and 50 μg mL^{-1} of free VWF are averages over 48, 170, and 166 tethered VWF concatemers, respectively.

dissociated at a slower rate of ~0.02 s^{-1} in the presence of 10 μg mL^{-1} free VWF (Figure 1E). About 4% of bound VWF did not dissociate after ~5 minutes. After initial binding of free VWF to tethered VWF, some bound molecules may become photodamaged. Therefore, the minor population of slowly dissociating molecules could be, at least in part, artificial.

Tension regulates VWF self-association

To further study the role of tension in VWF self-association, we measured binding kinetics as a function of tensile force within tethered VWF. At each point along a tethered VWF molecule, mechanical tension is approximately proportional to the number of monomers downstream on which hydrodynamic drag force is exerted. The drag force was estimated as 0.38 pN per monomer at 960 dyn cm^{-2}.[6] Hence, tensile force along the VWF spine is maximal at the tether point and decreases linearly to zero at the downstream end. The time trace of binding at 10 μg mL^{-1} free VWF in each tension bin (Figure 2A) was used to calculate binding kinetics (Figure 2B). Only tethered VWF molecules that were long enough to include a 40 to 60 pN force bin at 960 dyn cm^{-2} were included in the tension-based data analysis. Over time, binding of free VWF adds extra drag force to the tethered VWF molecule and thus increases tensile force between the tether point and the point(s) at which free VWF binds. Uncertainties in the number and location of binding sites between the tethered and bound VWF molecules and heterogeneity in the evolution of the tension profile among individual tethered VWF molecules prevented us from precisely taking these factors into account in our calculations. Therefore, we used the initial tension profile in tethered VWF before binding of free VWF and analyzed binding rates within the initial time period of binding at each flow rate to minimize the effects of bound VWF on further VWF binding (supplemental Methods).

We used two measures of free VWF binding to tethered VWF. Binding kinetics were measured in the initial linear regime of the first 10 seconds of the 35-second binding periods for 10 μg mL^{-1} free VWF at 960 dyn cm^{-2}. We also measured final binding density by averaging bound VWF monomer numbers per μm of tethered VWF at 33 to 35 seconds. Both measures increased markedly between the 0 to 10 and the 20 to 30 pN force bins (ie, from about 5 to 25 pN) and then plateaued between 25 and 50 pN (Figure 2A-C). To take a closer look at the force range below the plateau, we used 5 pN rather than 10 pN tension bins to analyze initial binding rates at 480 dyn cm^{-2} (Figure 2D). The rate was low at 0 to 5 pN, sharply increased between the 5 to 10 and the 15 to 20 pN bins, and plateaued at the 15 to 20 and 20 to 25 pN bins. This sigmoid trend matches a 2-state model. Therefore, we fit our data to a model in which a site in VWF that does not bind, or binds slowly, is activated by force to a site that binds rapidly and presumably with high affinity (Figure 2E-F). Fits to data at 480 and 960 dyn cm^{-2} gave maximal binding rates and half maximal accumulation (f_{50}) values within experimental error estimatesof one another and in agreement with simple interpolation from the results. The data at 480 dyn cm^{-2} showed more points at low force (the 0-5 and 5-10 pN bins) where binding was low, which therefore better emphasized the high tension required to activate binding kinetics and resulted in a larger ΔG value. Although

neither Δx or ΔG have been precisely determined, they illustrate the range of possible values allowed by our data.

Complexities of VWF self-association

Accumulation of VWF in flow on tethered VWF has multiple complexities. VWF concatemers have many monomers, and thus binding may involve multivalent interactions between multiple monomers in both the tethered and bound VWF concatemers (Figure 3A). Furthermore, once VWF in flow binds, it provides additional secondary VWF binding sites that increase the total tension on the primary tethered VWF concatemer. However, if primary and secondary VWF bind to one another at multiple sites, few secondary VWF monomers would be downstream of each interaction site, limiting tension buildup on secondary VWF. At the same time, secondary VWF could block access to primary VWF and inhibit further accumulation (Figure 3A).

These complexities were reflected in concentration-dependent VWF accumulation (Figure 3B). Over a range of VWF concentrations, accumulation at 480 and 960 dyn cm^{-2} was faster in the first half of the accumulation period than in the second half. This is an important observation, because if VWF accumulated from the flow stream was as effective as tethered VWF for the accumulation of more VWF, the rate of accumulation would accelerate instead of slowing as observed. The slowing of the rate of binding is similar to what is observed in saturation binding; however, only a few monomers with force-activated binding sites within tethered VWF might suffice to bind VWF in flow; therefore, saturation binding may not be the correct explanation. The ability of tethered VWF to bind more than its own mass of VWF is illustrated by binding after 35 seconds at 960 dyn cm^{-2} of 1.5-fold more mass from the flow stream at 50 μg mL^{-1} (Figure 3B).

To quantitatively examine these complexities, we studied accumulation at 960 dyn cm^{-2} with time as a function of both free VWF concentration and tension bin within the tethered VWF (Figure 4A, unbroken lines). The initial rate of binding and total accumulation increased as VWF concentration increased from 1 to 50 μg mL^{-1} in all tension bins (Figure 4A). At the highest tension bin of 40 to 60 pN, binding of VWF at 10 μg mL^{-1} was still increasing after 30 seconds and at 35 seconds, it reached 40.1 ± 2.5 bound monomers per μm of tethered VWF; at 50 μg mL^{-1} of VWF, binding reached 77.5 ± 0.9 bound monomers per μm at 35 seconds (Figure 4A). Binding in the 40-to-60 pN bin corresponded to bound or tethered VWF mass ratios of 1.1 ± 0.1 and 2.00 ± 0.02 at 10 and 50 μg mL^{-1}, respectively, and agrees with the ability of tethered VWF to bind more than its own mass of free VWF as shown in Figure 3. The free VWF binding kinetics deviated from a simple homogeneous 1:1 binding model. Globally fitting our binding kinetics measurements in each tension bin and at each VWF concentration to such a model only partially matched the results (Figure 4A, dashed lines), likely the result of the complexities discussed in this section.

Therefore, to minimize the effects of free VWF accumulation, we quantified the initial free VWF binding rate k_{obs} at the first 35, 20, and 10 seconds for 1, 5, and 10 μg mL^{-1} of free VWF, respectively. We omitted the binding rates at 50 μg mL^{-1} where the greatest amount of VWF accumulation occurred and fit k_{obs} to a linear function of free VWF concentration at 0 to 10 μg mL^{-1} (Figure 4B). Fitting to our experimental data yielded the force-dependent slope a(*f*). a(*f*) increased with tension and reached a plateau at (5.8 ± 1.3) × 10^{-14} mL μm^{-1} s^{-1} above 25 pN (Figure 4C). The value of the parameter a(*f*) plateaued in the 20-to-30-pN tension bin and above, and the f_{50} value of 11.5 ± 0.6 pN (Figure 4C) was consistent with f_{50} values from other measurements (Figure 2).

Coexistence of VWF self-association and GPIbα binding

Because the VWF A1 domain binds platelet GPIbα and has also been implicated in VWF self-association,[1,2,14] we examined the effects of VWF self-association on GPIbα binding and the effect of GPIbα binding on VWF self-association. We measured the binding of Alexa Fluor 647–labeled GPIbα to Alexa Fluor 488–labeled tethered VWF in the presence of varying concentrations of unlabeled free VWF at 960 dyn cm^{-2}. High-affinity GPIbα with G233V and M239V gain-of-function mutations found in patients with platelet-type von Willebrand disease was used to achieve a high signal-to-noise ratio.[7,17] The fluorescence intensity of bound GPIbα increased rapidly and plateaued after about 10 seconds of flow at 960 dyn cm^{-2} (Figure 5A). The binding of GPIbα was highly tension dependent, as previously described.[6] However, if free VWF was present at 0, 10, or 50 μg mL^{-1}, it had little effect on GPIbα binding whether binding was measured at 1.5 to 2.5 seconds or at 27 to 35 seconds (Figure 5B-C).

Conversely, we measured the binding of Alexa Fluor 647–labeled free VWF to Alexa Fluor 488–labeled tethered VWF in the presence of 200 nM unlabeled high-affinity GPIbα, a concentration that is 33-fold higher than its ~6 nM K_d for mechanically tensioned VWF above 30 pN.[7] A small but significant amount of inhibition of VWF self-association was observed (supplemental Figure 1). The ARC1172 aptamer binds to a site on A1 that overlaps with the GPIbα binding site on A1, and ARC1172 completely inhibits GPIbα binding.[19,20] ARC1172 at 60 nM, a concentration 100-fold higher than its 0.6 nM K_d for A1[19] also modestly but significantly inhibited VWF self-association (supplemental Figure 2). However, the small amount of inhibition by these competitors, despite their use at levels much higher than their K_d values, suggests that they affect self-association by a mechanism other than competing for the same binding site.

Discussion

Our measurements provide important insights into how circulating plasma VWF associates with VWF tethered to the blood vessel wall to regulate hemostasis and thrombosis. We reconstituted the process of VWF self-association on single tethered VWF concatemers in shear flow and directly measured the kinetics and the effect of tension on this process. To bind free VWF, we found that tethered VWF must not only elongate from a compact, random coil state[21] to an extended form but also reach a tension of 10 pN for half maximal accumulation (the f_{50} value). Accumulation plateaued at forces above 20 pN.

Flow applies a hydrodynamic force to tethered VWF molecules, inducing mechanical tension within them. The flow-induced mechanical tension is highest at the tether point and decreases linearly to zero at the downstream end of the tethered VWF concatemer. This tension distribution was reflected in the localized pattern of VWF binding from the flow stream. Tethered VWF was extended by shear flow in our basal condition of 80 dyn cm^{-2}, yet binding of free VWF was not detected. The binding was barely detectable at 240 dyn cm^{-2}, was marked at 480 dyn cm^{-2}, and was greater at 960 dyn cm^{-2}. The latter two wall shear stresses are not found physiologically and are expected to be present only during excessive blood flow at sites of bleeding, especially with the vasoconstriction that accompanies vessel injury, or in pathologies including stenosis.[6] Alternatively, at physiologic shear stresses, binding of platelets to tethered VWF would increase mechanical tension and bring it into the range required for VWF self-association.

One tethered VWF concatemer could bind multiple concatemers from the flow stream. Tethered VWF molecules were observed to bind more than their own mass of VWF molecules from the flow stream, showing that self-association has the potential to amplify hemostasis and thrombosis. The multimeric nature of a VWF concatemer is important for it to bind multiple other concatemers, just as a single concatemer could bind multiple platelets. Multiple attachments might form between a primary and a bound (secondary) concatemer (Figure 3A). If so, this would minimize the tension in secondary VWF molecules, because only monomers between each attachment point would contribute tension to the upstream attachment point.

Theoretically, VWF bound from the flow stream (secondary VWF) could have the capability of binding more VWF (tertiary VWF). This would cause binding from the flow stream to accelerate; however, the opposite occurred, that is, the rate of binding decreased. Conversely, VWF binding did not become saturated on our experimental time scale, even after accumulation of more than 1.5 times the mass of the tethered VWF. Saturation of binding sites may be one of the factors that slowed VWF accumulation, even though only a small proportion of VWF monomers in both concatemers may be required for binding. Another factor would be limitation by multipoint binding of tensile force on secondary VWF, as discussed in the previous paragraph. Secondary bound VWF would apply additional tension to primary tethered VWF, and it would also partially shield it from binding more secondary VWF, and thus could contribute to the decrease in the rate of VWF binding (Figure 3B). In contrast to the small GPIbα ectodomain, substantial hydrodynamic force is applied to a secondary VWF concatemer, which could help break VWF self-association bonds. Thus, force-promoted dissociation may also contribute to slowing of accumulation described in the previous paragraph.

When flow was returned to our baseline 80 dyn cm^{-2} wall shear stress, most bound VWF rapidly dissociated from VWF tethers even though the tethers remained extended. This finding emphasized that VWF self-association was noncovalent and completely distinct from the covalent disulfide bonds that link VWF monomers head-to-head and tail-to-tail into concatemers. Like VWF, GPIbα extracellular fragments also rapidly dissociated from tethered VWF when flow, and hence mechanical tension, were lowered below a threshold.[6]

Tethered VWF may be found in vivo at vascular sites of stimulated secretion from endothelial cells or of damage that exposes subendothelial collagen for VWF binding. The average single VWF concatemers studied here were 3.6 ± 1.1 μm in length at 960 dyn cm^{-2}. VWF tubules stored in Weibel-Palade bodies can be as long as 5 μm. Each is thought to contain a single VWF concatemer with a maximal extension of ~250 μm.[2] Therefore, as a VWF concatemer is being extruded during secretion, it could form a tether with a length much longer than any studied here, with a correspondingly higher tension within it.

The A1 and A2 domains are known to be responsive to mechanical tension in VWF concatemers and are plausible binding sites in VWF self-association. Therefore, it is intriguing to compare the force requirements for VWF self-association found here with those previously found for VWF A1 domain binding to GPIb[6,22,23] and for A2 domain unfolding.[24-26] Most previous measurements differed from our measurements in being force ramp experiments, in which force was linearly increased until an event occurred. In contrast, we measured VWF binding frequencies as a function of a constant flow rate within bins of constant tension. Thus, the dependence on force of the equilibrium between active and inactive sites for self-association in the tethered VWF was measured here. The f_{50} value of 10 pN measured here for activation of the site(s) for self-association corresponds to the force at which the rates of activation and inactivation are equal. Reversibility was established by dissociation of secondary VWF when the flow rate was lowered to 80 dyn cm^{-2}. Among the previous measurements cited in this paragraph, only one study is directly comparable, and it showed that the equilibrium between binding and unbinding of GPIb to the A1 domain of VWF occurred with an f_{50} value of 20 pN.[6] The large difference from the f_{50} value of 10 pN for VWF self-association strongly suggests that GPIb binding and VWF binding are activated by distinct mechanisms. This is in agreement with the failure of GPIb and ARC1172 to have more than a modest effect on VWF self-association, which suggests that their binding sites do not overlap with the binding site for VWF self-association and that they may inhibit by an indirect mechanism such as binding to a nearby site.

A2 domain unfolding is difficult to compare with our f_{50} value because the peak of the force distribution for A2 unfolding was measured during force ramp experiments,[24-26] and the peak force is proportional to the log of the rate of force increase.[27,28] The A2 domain seemed to be stabilized by its neighbors, because at a force ramp of 22 pN s^{-1}, it unfolded at 11 pN as an isolated A2 domain and at 22 and 23 pN in intact VWF, and in $(A1A2A3)_3$ concatemers, respectively.[24,25] Refolding of isolated A2 occurred in ~3 seconds at 1 pN.[24] If A2 refolding was also stabilized by its A1 and A3 neighbors, then it might be possible that in intact VWF, the rates of A2 unfolding and refolding would be equal at ~10 pN, as would be required for the unfolded A2 domain to be a candidate for the binding site for VWF self-association. However, our experiments in shear flow (here and in Fu et al[6]) use an estimate of the force calculated from fluid dynamics rather than more direct measurements based on calibrations.[24,25] It will be important to test A2 and other domains in VWF as possible sites for self-association in the primary VWF concatemer. It also is important to define the binding site(s) in the secondary VWF concatemer for self-association. The ability of mechanical tension to activate VWF binding shows

that the active state is more extended than the inactive state, which would be the case for the unfolded A2 domain and for other mechanically sensitive domains that have high-affinity folded states that are more extended than low-affinity folded states.[29-31]

Our direct measurements here of VWF self-association in shear flow allow this process to be understood more fully in the overall process of formation of the VWF-platelet plug in vivo. The force-dependent unfolding of the A2 domain exposes tethered VWF to cleavage by the protease ADAMTS13, which would liberate VWF fragments downstream of the cleavage site into the flow stream and also decrease the tension on the remaining upstream fragment. In contrast, binding of platelets and VWF in the flow stream to tethered VWF increases tension on the tethered VWF. Furthermore, our finding that VWF binding from the flow stream did not accelerate further accumulation of VWF suggests an inherent feature in VWF that limits its self-association and prevents an uncontrolled chain reaction, even in the absence of physiological regulation such as by ADAMTS13 cleavage.

Shear-dependent VWF self-association has previously been investigated in complex systems involving platelet-VWF as well as VWF-VWF interactions and interactions in whole blood.[8-14] The single-molecule assay developed here goes to the heart of VWF self-association by probing the VWF-VWF interaction directly and has revealed its dependence on mechanical tension within tethered VWF, association kinetics, and reversal when mechanical tension is lowered. The similar yet distinct ranges of the tensions required for self-association, activation of the high-affinity state of VWF A1 for GPIbα, and unfolding of A2 for cleavage by ADAMTS13 allow hemostasis and thrombosis to be exquisitely sensitive to rapid changes in blood flow at a site of hemostasis or thrombosis. However, much more remains to be learned about the identity of domains in tethered VWF and VWF in the flow stream that associate with one another and the mechanism by which tension induces binding, presumably by stabilizing a more extended conformation of a domain within VWF. Because VWF is multimeric, it is possible that self-association involves contacts between multiple monomers in each concatemer. Finally, it will be important to find agents that completely inhibit self-association to better define its molecular mechanism and to test as therapeutics in thrombosis.

Acknowledgments

The authors acknowledge help from the microfluidic prototyping facilities at the Wyss Institute for Biologically Inspired Engineering at Harvard University.

This work was supported by grants from the National Institutes of Health (NIH), National Heart, Lung, and Blood Institute (K25HL135432 [H.F.], K25HL146949 [Y.J.], and R01HL148755 [T.A.S.]) NIH, National Institute of General Medical Sciences (R35 GM119537) (W.P.W.), and an ASH Scholar Award (H.F.).

Authorship

Contribution: T.A.S., W.P.W., H.F., and Y.J. designed the research and drafted the manuscript; H.F. and Y.J. performed the experiments; and T.A.S., W.P.W., H.F., and Y.J. analyzed the data.

Conflict-of-interest disclosure: The authors declare no competing financial interests.

ORCID profiles: H.F., 0000-0002-6893-8260; Y.J., 0000-0002-2745-4323; W.P.W., 0000-0001-7398-546X; T.A.S., 0000-0001-6627-2904.

Correspondence: Timothy A. Springer, Center for Life Sciences, Room 3103, Boston Children's Hospital, 3 Blackfan Circle, Boston, MA 02115; e-mail: springer@crystal.harvard.edu; and Wesley P. Wong, Center for Life Sciences, 3rd Floor, Boston Children's Hospital, 3 Blackfan Circle, Boston, MA 02115; e-mail: wesley.wong@childrens.harvard.edu.

Footnotes

Submitted May 19, 2021; accepted July 22, 2021; prepublished online on *Blood* First Edition August 19, 2021. DOI 10.1182/blood.2021012595.

*H.F. and Y.J. contributed equally to this study.

Data generated by this study are available upon request to the corresponding authors. The DNA construct for recombinant GPIbα is available in Addgene.

The online version of this article contains a data supplement.

There is a *Blood* Commentary on this article in this issue.

The publication costs of this article were defrayed in part by page charge payment. Therefore, and solely to indicate this fact, this article is hereby marked "advertisement" in accordance with 18 USC section 1734.

REFERENCES

1. Sadler JE. Biochemistry and genetics of von Willebrand factor. *Annu Rev Biochem.* 1998; 67(1):395-424.
2. Springer TA. von Willebrand factor, Jedi knight of the bloodstream. *Blood.* 2014; 124(9):1412-1425.
3. Sadler JE. New concepts in von Willebrand disease. *Annu Rev Med.* 2005;56(1):173-191.
4. Savage B, Almus-Jacobs F, Ruggeri ZM. Specific synergy of multiple substrate-receptor interactions in platelet thrombus formation under flow. *Cell.* 1998;94(5):657-666.
5. Reininger AJ. Function of von Willebrand factor in haemostasis and thrombosis. *Haemophilia.* 2008;14(suppl 5):11-26.
6. Fu H, Jiang Y, Yang D, Scheiflinger F, Wong WP, Springer TA. Flow-induced elongation of von Willebrand factor precedes tension-dependent activation. *Nat Commun.* 2017; 8(1):324.
7. Jiang Y, Fu H, Springer TA, Wong WP. Electrostatic steering enables flow-activated von Willebrand factor to bind platelet glycoprotein, revealed by single-molecule stretching and imaging. *J Mol Biol.* 2019;431(7): 1380-1396.
8. Savage B, Sixma JJ, Ruggeri ZM. Functional self-association of von Willebrand factor during platelet adhesion under flow. *Proc Natl Acad Sci U S A.* 2002;99(1):425-430.
9. Shankaran H, Alexandridis P, Neelamegham S. Aspects of hydrodynamic shear regulating shear-induced platelet activation and self-association of von Willebrand factor in suspension. *Blood.* 2003;101(7):2637-2645.
10. Ulrichts H, Vanhoorelbeke K, Girma JP, Lenting PJ, Vauterin S, Deckmyn H. The von Willebrand factor self-association is modulated by a multiple domain interaction. *J Thromb Haemost* 2005;3(3):552-561.
11. Barg A, Ossig R, Goerge T, et al. Soluble plasma-derived von Willebrand factor assembles to a haemostatically active filamentous network. *Thromb Haemost.* 2007; 97(4):514-526.
12. Dayananda KM, Singh I, Mondal N, Neelamegham S. von Willebrand factor self-association on platelet Gplbalpha under hydrodynamic shear: effect on shear-induced platelet activation. *Blood.* 2010; 116(19):3990-3998.

13. Chung DW, Chen J, Ling M, et al. High-density lipoprotein modulates thrombosis by preventing von Willebrand factor self-association and subsequent platelet adhesion. *Blood*. 2016;127(5):637-645.

14. Zhang C, Kelkar A, Neelamegham S. von Willebrand factor self-association is regulated by the shear-dependent unfolding of the A2 domain. *Blood Adv*. 2019;3(7):957-968.

15. Yuan H, Deng N, Zhang S, et al. The unfolded von Willebrand factor response in bloodstream: the self-association perspective. *J Hematol Oncol*. 2012;5(1):65.

16. López JA, Chung DW. VWF self-association: more bands for the buck. *Blood*. 2010;116(19):3693-3694.

17. Blenner MA, Dong X, Springer TA. Structural basis of regulation of von Willebrand factor binding to glycoprotein Ib. *J Biol Chem*. 2014;289(9):5565-5579.

18. Handin RI, Lux SE, Stossel TP, eds. Blood: Principles and Practice of Hematology. 2nd ed. Philadelphia, PA: Lippincott Williams & Wilkins; 2003

19. Huang RH, Fremont DH, Diener JL, Schaub RG, Sadler JE. A structural explanation for the antithrombotic activity of ARC1172, a DNA aptamer that binds von Willebrand factor domain A1. *Structure*. 2009;17(11):1476-1484.

20. Diener JL, Daniel Lagassé HA, Duerschmied D, et al. Inhibition of von Willebrand factor-mediated platelet activation and thrombosis by the anti-von Willebrand factor A1-domain aptamer ARC1779. *J Thromb Haemost*. 2009;7(7):1155-1162.

21. Parker ET, Lollar P. Conformation of the von Willebrand factor/factor VIII complex in quasi-static flow. *J Biol Chem*. 2021;296:100420.

22. Kim J, Zhang CZ, Zhang X, Springer TA. A mechanically stabilized receptor-ligand flex-bond important in the vasculature. *Nature*. 2010;466(7309):992-995.

23. Ju L, Dong JF, Cruz MA, Zhu C. The N-terminal flanking region of the A1 domain regulates the force-dependent binding of von Willebrand factor to platelet glycoprotein Ibα. *J Biol Chem*. 2013;288(45):32289-32301.

24. Zhang X, Halvorsen K, Zhang CZ, Wong WP, Springer TA. Mechanoenzymatic cleavage of the ultralarge vascular protein von Willebrand factor. *Science*. 2009;324(5932):1330-1334.

25 Ying J, Ling Y, Westfield LA, Sadler JE, Shao J-Y. Unfolding the A2 domain of von Willebrand factor with the optical trap. *Biophys J*. 2010;98(8):1685-1693.

26 Wu T, Lin J, Cruz MA, Dong JF, Zhu C. Force-induced cleavage of single VWF A1A2A3-tridomains by ADAMTS-13. *Blood*. 2010;115(2):370-378.

27. Evans E, Ritchie K. Dynamic strength of molecular adhesion bonds. *Biophys J*. 1997;72(4):1541-1555.

28. Dudko OK, Hummer G, Szabo A. Intrinsic rates and activation free energies from single-molecule pulling experiments. *Phys Rev Lett*. 2006;96(10):108101-108104.

29. Astrof NS, Salas A, Shimaoka M, Chen J, Springer TA. Importance of force linkage in mechanochemistry of adhesion receptors. *Biochemistry*. 2006;45(50):15020-15028.

30. Springer TA. Structural basis for selectin mechanochemistry. *Proc Natl Acad Sci U S A*. 2009;106(1):91-96.

31. Yakovenko O, Tchesnokova V, Sokurenko EV, Thomas WE. Inactive conformation enhances binding function in physiological conditions. *Proc Natl Acad Sci U S A*. 2015;112(32):9884-9889.